STRAIGHTENING OF A WAVY STRIP - AN ELASTIC-PLASTIC CONTACT PROBLEM INCLUDING SNAP-THROUGH

Dieter F. Fischer and Franz G. Rammerstorfer
VOEST-ALPINE AG, FAT, Linz, Austria

SUMMARY

This paper deals with calculating the non-linear behaviour of a wave-like deformed metal strip during the levelling process. Elastic-plastic material behaviour as well as nonlinearities due to large deformations are considered. The considered problem leads to a combined stability and contact problem. It is shown that, despite of the initially concentrated loading, neglecting the change of loading conditions due to altered contact domains may lead to a significant error in the evaluation of the nonlinear behaviour and particularly to an underestimation of the stability limit load. The stability is examined by considering the load deflection path and the behaviour of a load-dependent current stiffness parameter in combination with the determinant of the current stiffness matrix.

INTRODUCTION

The stability of nonlinear structures is the goal of many recent papers. Especially the snap-through behaviour of initially curved slender bars has been analytically as well as numerically considered (e.g. ref. 1,2). But investigations in which the influence of contact between the loading and the loaded structures is considered are rather rare. Such a combined contact and stability problem will be treated in this paper. In order to show how the loading conditions influence the nonlinear behaviour and the stability limit in particular, let us draw our attention to the following simple example.

Figure 1 shows a shallow circular arch which is loaded once directly by a concentrated load and in a second case by a rigid horizontal plane plate moved towards the arch. The latter is treated as a contact problem. In both cases, symmetry with respect to the vertical axis is assumed for simplicity.

Applying the algorithm which is described later we get results shown in figure 2. In figure 2 the load displacement path, $P(w)$, the dependence of the normalized determinant of the current stiffness matrix, $\det_n \underline{K}(P)$, and of the current stiffness parameter (ref. 3,4), $CS(P)$, on the applied load, P, is described. In both cases, distinct snap-through behaviour can be observed by considering the final tangent of the $\det_n \underline{K}(P)$ curve which crosses the P-axis perpendicularly (ref. 5). Also the vanishing current stiffness parameter, CS, indicates snap-through. However in the case b (load application by a rigid plate) a significantly higher stability limit than in case a was found. Thus,

it is important to recognize the altering loading conditions even if the load is applied at a single point in the initial state (i.e. at a very low load level). The problem being dealt with in the following chapters is a typical stability and contact problem.

DESCRIPTION OF THE WAVED STRIP PROBLEM

The behaviour of an infinite strip with periodic wave-like initial out-of-plane deformations is investigated during a straightening process. Periodic out-of-plane deformations at the boundaries (fig. 3) or in the middle domain of the strip sometimes appear in metal sheets as a consequence of the rolling process. The straightening is based on plastic deformations caused by moving the strip through a leveller in which it is bent by rollers in a repeated manner. In some cases, a snap-through of the waves can be observed which renders an unsuccessful result of the levelling process. In order to find proper conditions for avoiding snap-through, a procedure for calculating the non-linear elastic-plastic stability problem was developed. The deformations during levelling are caused by rather stiff rollers. A contact problem has to be solved simultaneously with the stability problem in order to account for the stiffening effect due to expanded contact.

To approach the real behaviour of the waved strip during the levelling process by mathematical investigation, the complicated transient problem is simplified to a static consideration: The nonlinear behaviour of the shaded area of the strip in figure 3 under a downward moving rigid roller is calculated with the aid of the finite element method.

THE MATHEMATICAL MODEL

The following data were taken from an example in which instabilities in the practical levelling process were observed: B = 3500 mm, L = 1000 mm, S = 20 mm, t = 10 mm. The material is assumed to be elastic-plastic with linear strain hardening. The following material properties correspond to experimentally derived values at a temperature of 600 ^{o}C (the strip temperature during the levelling process): E = 180000 N/mm^2 (Youngs' modulus), ν = 0.3 (Poisson's ratio), σ_y = 130 N/mm^2 (initial yield stress), E_T = 5000 N/mm^2 (strain hardening modulus). The shaded area in figure 3 under consideration represents a doubly curved shallow shell which is modeled using ADINA shell elements (ref. 6). These elements allow for nonlinear material behaviour as well as geometric nonlinearities using the total Lagrangian formulation. Figure 4 shows the finite element model.

The midsurface of the shell is approximated by

$$z(x,y) = S \frac{4y^2}{B^2} \sin \frac{(L-2x)\pi}{2L} . \qquad (1)$$

As shown in reference 7 the contact conditions can be verified with the aid of contact elements. These contact elements are simple truss elements

which have a certain nonlinear elastic material behaviour (figure 5).

The contact elements give only contributions to the global current stiffness matrix if the shell nodes to which they are attached belong to the contact area. They allow only transmission of compression forces corresponding to the contact pressure. Before a shell node becomes a contact point, the gap between the rigid roller and the shell surface must be closed. This is accounted for in the location-dependent activating strain, $\varepsilon_{gap}(y)$:

$$\varepsilon_{gap}(y) = - \frac{S - z(x=0,y)}{S + h - z(x=0,y)} \qquad (2)$$

The values of the tangent moduli, E_1, E_2, the stresses, σ_1^* and σ_2^*, the fictitious length, h, and the cross section area, A, of the contact elements must be properly chosen. This means that the contact elements should be stiff enough to prevent the roller from penetrating in the shell and, that the properties must not lead to a numerical instability of the incremental-iterative algorithms described below. The following values appear in the presented analysis: $E_1 = 1000\ N/mm^2$, $E_2 = 7500\ N/mm^2$, $\sigma_1^* = -5\ N/mm^2$, $\sigma_2^* = -20\ N/mm^2$, $h = 80\ mm$, $A = 1000\ mm^2$. These values render a well-conditioned system of equations. If one would like to regard the local compressibility of the roller, a certain choice of the σ-ε-behaviour of the contact elements would make it possible. Furthermore, bending deformations of the roller could be considered, if beam elements would represent the axis of the roller instead of the rigid line $\overline{BC}$ (figure 4). Both effects, local compressibility and bending of the roller, are negligible in the investigated example.

In order to represent the periodicity of the structure, the boundary conditions of the finite element model are introduced as shown in figure 4. The waved strip will elongate globally due to the levelling process. For the x-displacement at the boundary $x = L/2$ the following restriction is valid: $u_x(x=L/2,y) = u_x(x=L/2,y=0)$.

DESCRIPTION OF THE ALGORITHMS

The analysis is performed in an incremental-iterative manner, using the tangent stiffness matrix concept and the BFGS iteration procedure as described elsewhere, e.g. in references 8,9. Let us concentrate our attention to the stability algorithms. Algorithms which treat nonlinear stability problems as a sequence of eigenvalue problems are described in recent papers (e.g. ref. 10 - 12). Let us now use the normalized determinant of the current tangent stiffness matrix, $\det_n \underline{K}$, and the current stiffness parameter, CS, recently introduced by Bergan (ref. 3,4) as indicators for the stability behaviour of the structure during the lowering of the rigid roller. It is a well-known fact that at the stability limit, $\lambda \rightarrow \lambda_{crit}$ (λ... load amplifier, λ_{crit}... critical load amplifier), the determinant of the tangent stiffness matrix vanishes:

$$\lim_{\lambda \rightarrow \lambda_{crit}} \det \underline{K}(\lambda) = 0. \qquad (3)$$

This criterion holds for both buckling as well as snap-through because it is based on the existence of a nontrival solution $\underline{\delta_u}$ of the equation

$$\underline{K}(\lambda_{crit}) \cdot \underline{\delta_u} = \vec{0}, \tag{4}$$

valid at the bifurcation point and at the snap-through point.

One can distinguish between buckling and snap-through by considering how the determinant approaches zero (ref. 5,10): In the buckling case

$$\lim_{\lambda \to \lambda_{crit}} \frac{\partial \det K}{\partial \lambda} = (-\infty, 0) \tag{5}$$

holds. If the determinant behaves according to

$$\lim_{\lambda \to \lambda_{crit}} \frac{\partial \det K}{\partial \lambda} = -\infty \tag{6}$$

snap-through is indicated.

The Gauss elimination procedure which is implemented in ADINA (ref. 6) is used in combination with the LDL^T fractorization (ref. 13) to solve the finite element equation system during the incremental-iterative analysis. Thus, it is almost no effort to calculate the determinant of the nxn stiffness matrix using the following relations:

$$\underline{K} = \underline{L}\,\underline{D}\,\underline{L}^T, \tag{7}$$

$\underline{L}$ is a lower unit triangular matrix and $\underline{D}$ is a diagonal matrix. Hence,

$$\det \underline{K} = \det \underline{D} = \prod_{i=1}^{n} D_{ii}. \tag{8}$$

This det $\underline{K}$ is normalized so that $\det_n \underline{K}(\lambda=0) = 1$. At each load level at which a further contact element is activated, the current global stiffness matrix increases suddenly due to the added contribution of the activated contact element. In order to avoid discontinuities in the $\det_n \underline{K}(\lambda)$ curve the current $\det_n$ values are smoothened by a further normalizing procedure which levels the $\det_n$ value just after a jump to that which appeared immediately before it. It might be proper to delete all contributions related to the contact elements from the current stiffness matrix if $\det_n \underline{K}(\lambda)$ is calculated. This would represent the determinant behaviour of the shell itself and the contact would only contribute to the load vector on the right-hand side of the incremental finite element equations.

The current stiffness parameter, ${}^{i}CS$, has the following meaning (i denotes the increment number): It represents the current stiffness of the structure as being a relation between a load increment and the corresponding displacement increment. Assuming proportional loading one can express

$${}^{i}\underline{R} = {}^{i}\lambda \underline{R}_{ref}. \tag{9}$$

${}^{i}\underline{R}$ denotes the external load vector at load level ${}^{i}\lambda$, $\underline{R}_{ref}$ is the constant reference load vector. Relating the current stiffness to the initial stiffness

(with ${}^{1}\lambda \ll 1$) ${}^{i}CS$ can be defined as

$$ {}^{i}CS = \frac{({}^{i}\lambda - {}^{i-1}\lambda)/\|{}^{i}\underline{u} - {}^{i-1}\underline{u}\|}{{}^{1}\lambda/\|{}^{1}\underline{u}\|} \tag{10} $$

using the Euclidean norm of the incremental displacement vector to scale the relations.

The combination of the determinant analysis and the current stiffness parameter calculation offers a good tool to predict the stability limit, λ_{crit}, as well as the instability mechanism (i.e. buckling or snap-through) as shown in reference 14.

DISCUSSION OF THE RESULTS

Figure 6 shows the load displacement path of the initial contact point (node A in figure 4), the normalized determinant of the stiffness matrix, $\det_n \underline{K}(\lambda)$, and the current stiffness parameter, $CS(\lambda)$. The results of the analysis of the same shell loaded by a concentrated load in A are also presented in figure 6 as a comparison. The following facts can be observed: In both cases a stability limit is reached and snap-through of the wave takes place. The shell loaded by the roller behaves significantly stiffer than the point-loaded shell. This is caused by the altering loading conditions due to the increasing contact domain as explained above. In the concentrated load approach, a horizontal tangent of the load displacement path is reached before considerable plastification takes place. In the contact solution, plastic domains appear in the vicinity of the contact area long before a significant stiffness loss (i.e. a rapid decrease of CS) can be observed.

In figure 7 the deformed state of the shell immediately before snap-through is shown. One can see that the contact domain between roller and strip is considerable. Furthermore, it is interesting to notice that the initial contact point A belongs no longer to the contact area.

CONCLUSION

From these considerations one can conclude that neglecting the change of loading conditions due to deformation dependent contact conditions may lead to an unnegligible error even if initially concentrated load conditions are justified.

REFERENCES

1. Pisanti, A.: Geometrically Nonlinear Behaviour of Initially Curved Plane Slender Bars and Frames. Inenieur-Archiv, Vol. 46, pp. 235 - 244, 1977.

2. Noor, A.K., Greene, W.H. and Hartley, S.J.: Nonlinear Finite Element Analysis of Curved Beams. Computer Methods Appl. Mech. Eng., Vol. 12, pp. 289 - 307, 1977.

3. Bergan, P.G., Horrigmoe, G., Kråkeland, B. and Søreide, T.H.: Solution Techniques for Non-Linear Finite Element Problems. Int. J. Numer. Methods Eng., Vol. 12, pp. 1677 - 1696, 1978.

4. Bergan, P.G.: Solution Algorithms for Nonlinear Structural Problems. Proc. Int. Conf. Eng. Appl. FEM, Høvik, Norway, 1979.

5. Gallagher, R.H. and Mau, S.: A Method of Limit Point Calculation in Finite Element Structural Analysis, NASA CR-2115, 1972.

6. Bathe, K.-J.: ADINA, A Finite Element Program for Automatic Dynamic Incremental Nonlinear Analysis, M.I.T. Report 82448-1, Acoustics and Vibration Laboratory, Mechanical Engineering Department, Mass. Inst. Techn., 1975 (Rev. 1978).

7. Rammerstorfer, F.G., Fischer, D. and Zitz, A.: Rock Bursting - A Nonlinear Dynamic Contact Problem, Num. Methods in Geomechanics, W. Wittke, A.A. Balkema, Rotterdam, 1979.

8. Bathe, K.-J., Bolourchi, S., Ramaswamy, S. and Snyder, M.D.: Some Computational Capabilities for Nonlinear Finite Element Analysis. Nucl. Eng. Design, Vol. 46, pp. 429 - 455, 1978.

9. Matthies, H. and Strang, G.: The Solution of Nonlinear Finite Element Equations, Int. J. Numer. Methods Eng., Vol. 14, pp. 1613 - 1626, 1979.

10. Ramm, E.: Geometrisch nichtlineare Elastostatik und finite Elemente, Habilitationsschrift, Univ. Stuttgart, 1975.

11. Brendel, B.: Geometrisch nichtlineare Elastostabilität, Bericht Nr. 79-1, Inst. f. Baustatik d. Univ. Stuttgart, 1979.

12. Brendel, B., Ramm, E., Fischer, D. and Rammerstorfer, F.G.: Linear and Nonlinear Stability Analysis of Thin Cylindrical Shells Under Wind Loads. To be published in J. Struct. Mech., Vol. 9, 1981.

13. Bathe, K.-J. and Wilson, E.L.: Numerical Methods in Finite Element Analysis, Prentice-Hall, Inc., Englewood Cliffs, New Jersey, 1976.

14. Rammerstorfer, F.G. and Fischer, D.F.: Nonlinear Elastic-Plastic Stability and Contact Problems Concerning the Straightening of a Wave-Like Deformed Strip Plate. Proc. 1st Int. Conf. Num. Methods for Non-Linear Problems, Swansea, Pineridge Press, 1980.

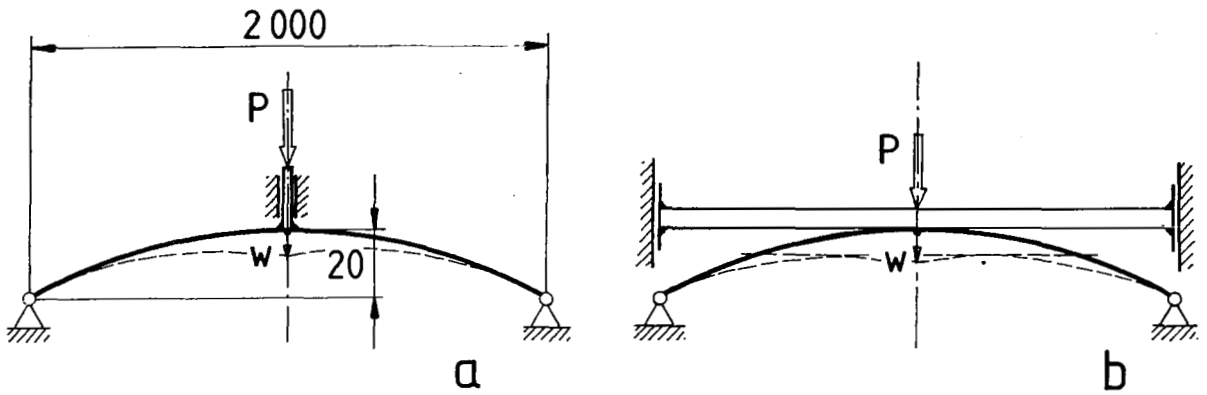

$EJ = 2.5 \times 10^{8}\ Nmm^{2}$

$EA = 3.0 \times 10^{7}\ N$

Figure 1.- The circular arch loaded by concentrated load directly (a) or via rigid plate (b).

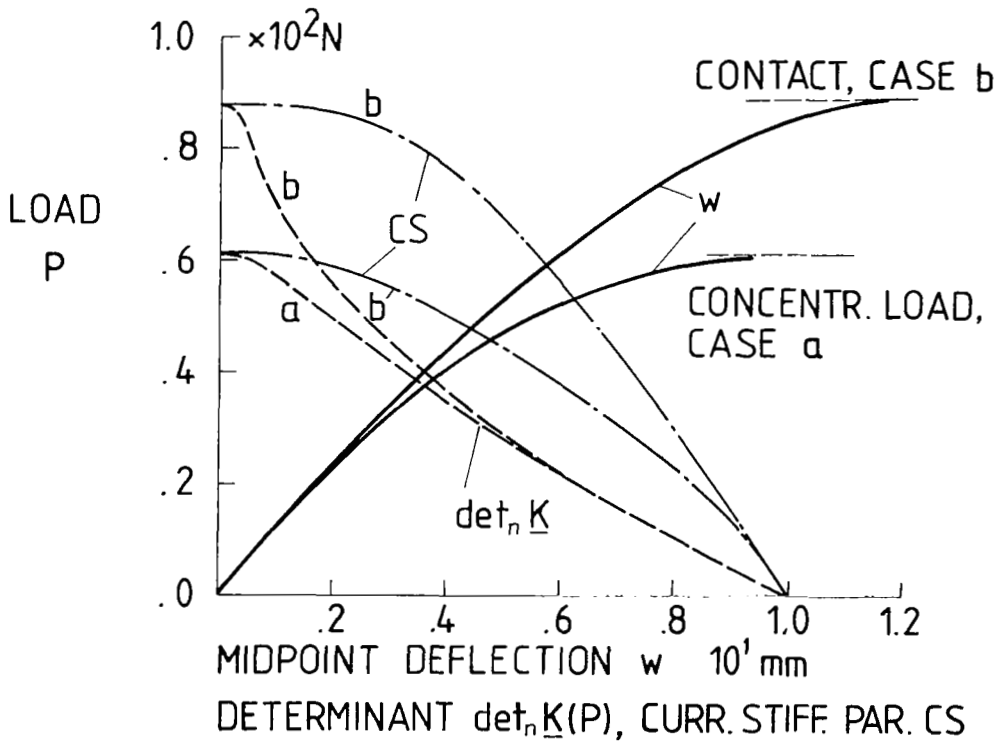

Figure 2.- Load displacement behaviour, normalized determinant of the current stiffness matrix and current stiffness parameter for the two different loading conditions.

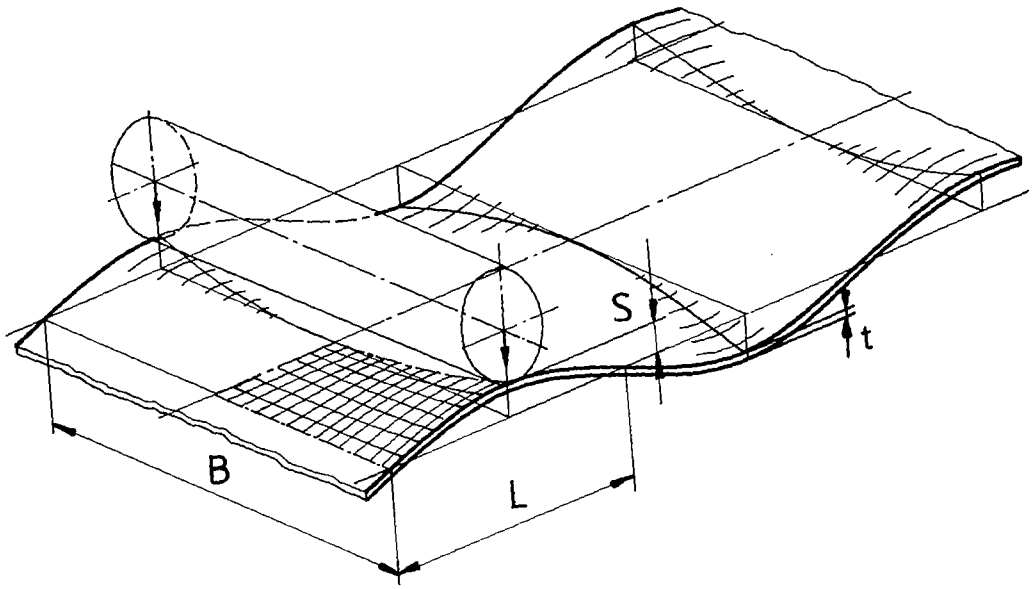

Figure 3.- The waved strip.

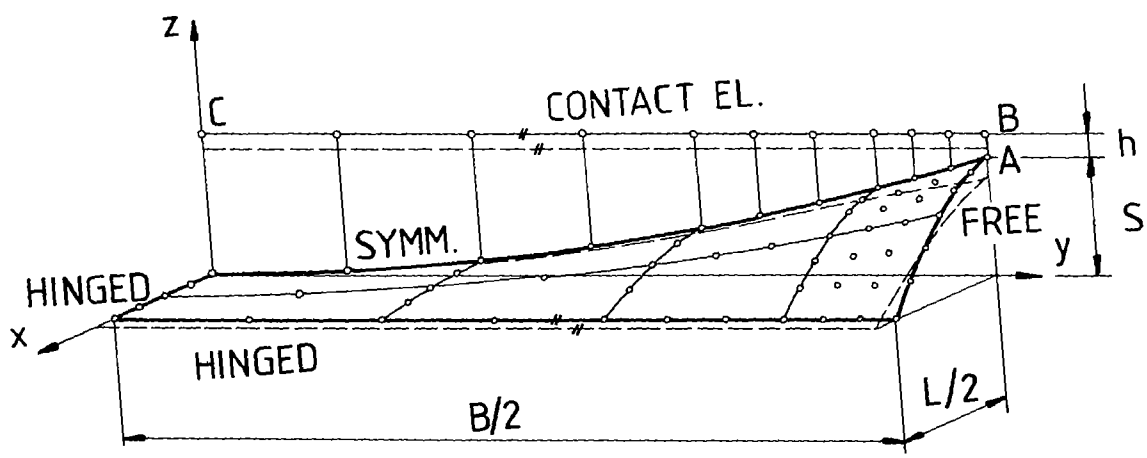

Figure 4.- The finite element model.

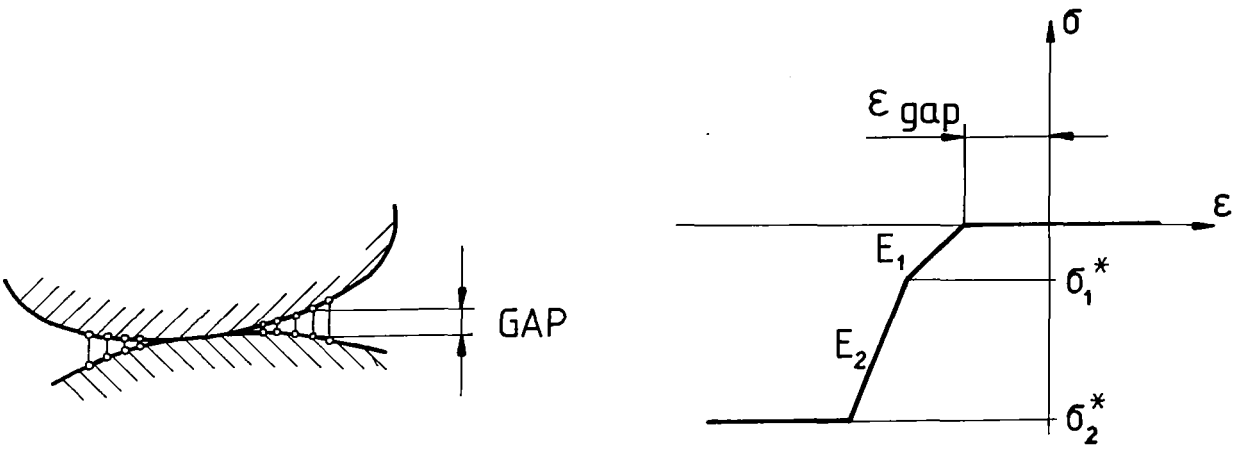

Figure 5.- Schematic sketch of the contact element material behaviour.

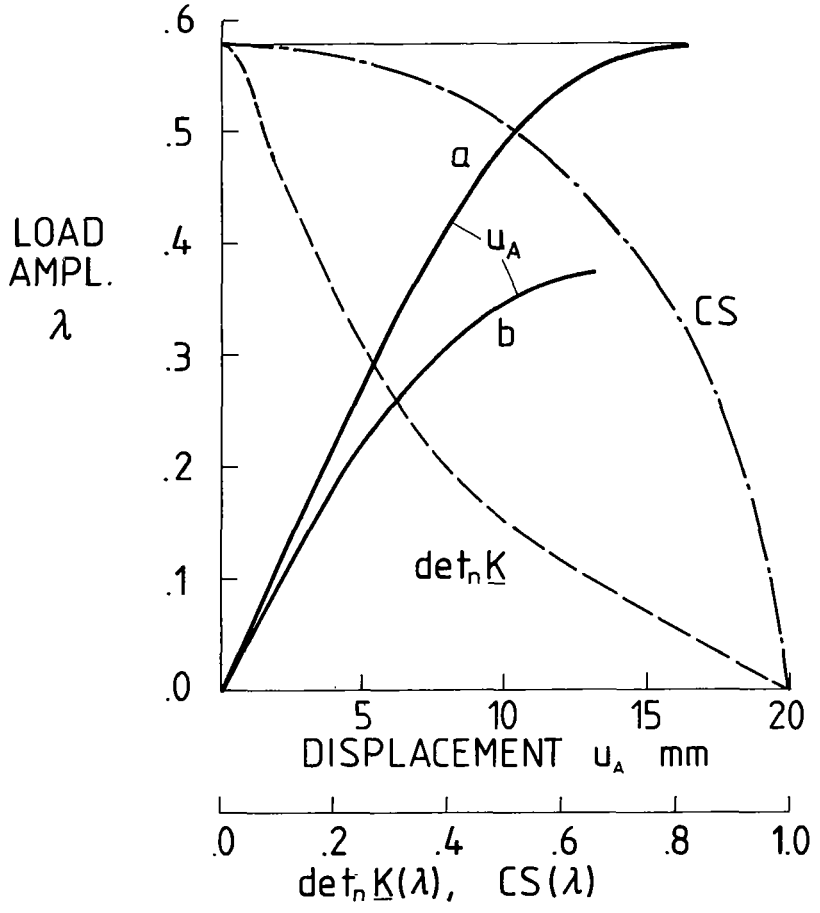

Figure 6.- Results of the analysis of the wavy strip plate obtained by (a) solving the contact problem and (b) concentrated load approach.

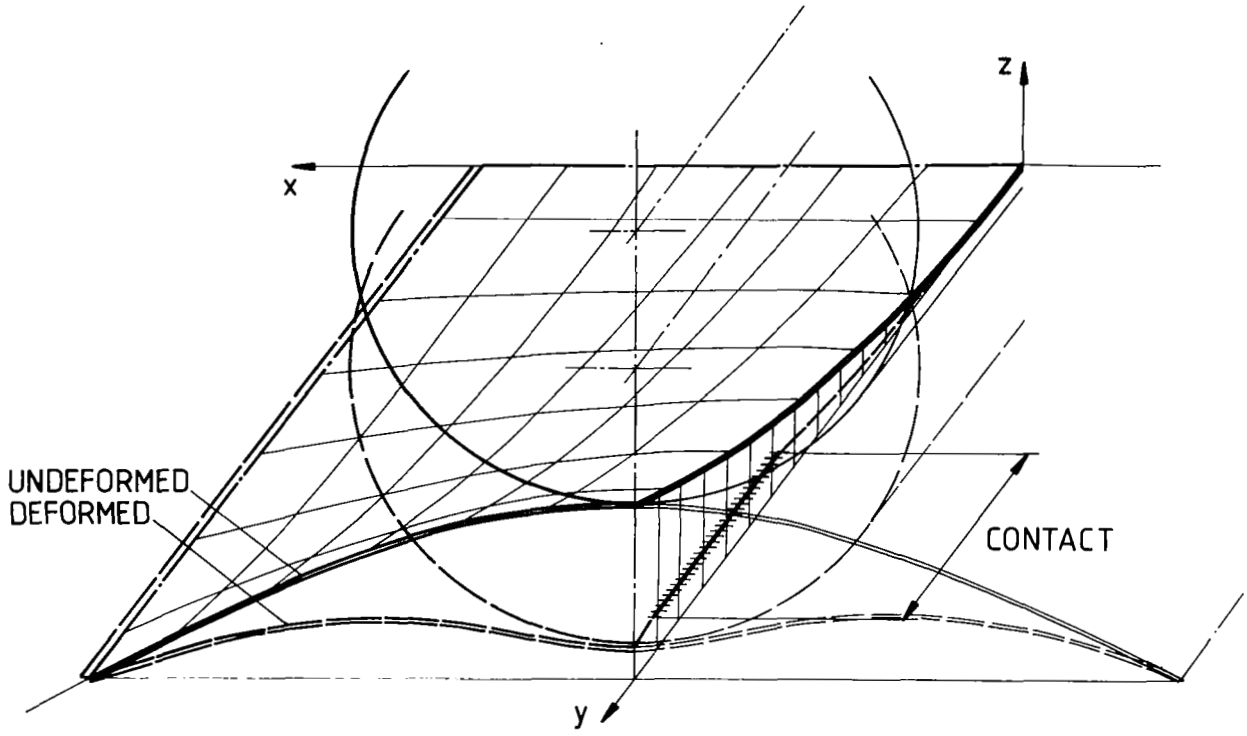

Figure 7.- Undeformed shell and configuration immediately before snap-through.